Acta Cryst. (1975). A31, 612

Experimental Measurements of the X-ray Scale Factor for Charge Density Studies

BY E. D. STEVENS AND P. COPPENS

Chemistry Department, State University of New York at Buffalo, Buffalo, New York 14214, *U.S.A.*

(*Received* 31 *January* 1975; *accepted* 26 *March* 1975)

Knowledge of the absolute values of X-ray intensities is highly desirable for a quantitative interpretation of experimental electron densities. In the present work X-ray scale factors are determined by three experimental methods. In the first method, a small aperture is used to measure the direct X-ray beam and the crystal volume is determined by weighing. In the second method, a single-crystal plate large enough to intercept the entire direct beam is used, while the third technique is based on powder diffraction intensity measurements. Scale factors are measured for orthorhombic sulfur, oxalic acid, glycylglycine, hexamethylenetetramine, sodium azide, and ammonium tetroxalate, all of which have been the object of previous electron density distribution studies. Results from the three methods agree within experimental errors and it is concluded that scale factors can be measured with an accuracy of about 1%. Comparison of the experimental scale with the results of various least-squares refinements indicates that scale factors from conventional least-squares refinements contain a considerable bias. Scale factors from refinements with improved models are generally in better agreement with experimental values. The effect of a variation in scale factor on the experimental electron densities is discussed.

Introduction

Accurate X-ray intensity measurements, when combined with positional and thermal parameters from neutron data or high-order X-ray data, can be used to calculate a difference density map which shows the redistribution of electron density in a molecule as compared with isolated atoms. Such studies have been the subject of a recent review (Coppens, 1974).

If the scale factor k is defined by

$$F(\text{obs}) = kF(\text{calc}) \tag{1}$$

then the difference density $\Delta\varrho$ is given by

$$\Delta\varrho = \frac{\varrho(\text{obs})}{k} - \varrho(\text{calc}), \tag{2}$$

where the calculated density subtracted out may represent all the electrons, only the core electrons or any other part of the density. An error in the scale factor k will bias the difference density, according to the expression

$$\mathrm{d}\left(\frac{\varrho(\text{obs})}{k}\right) = \frac{1}{k}\,\mathrm{d}[\varrho(\text{obs})] - \frac{\varrho(\text{obs})}{k^2}\,\mathrm{d}k \tag{3}$$

where ϱ(obs) does not include the contribution from $F(000)$.

Thus, a positive error in k will result in a negative bias in the difference density, which will be maximal near or at the nuclear positions where ϱ(obs) is large.

It is normal practice in crystallographic studies to determine the scale factor by least-squares refinement along with the positional and thermal parameters. However, refinements with different models may yield considerably different scale factors. Such differences are found, for example, between refinements with scattering factors based on Hartree–Fock (HF) and small-molecule optimized Slater-type orbitals (STO) (Stewart, 1970). As the scattering factors differ mainly in the low-order region the discrepancies decrease with decreasing thermal motion and increasing number of high-order data (Coppens, 1972).

In X-ray–neutron (X–N) studies the scale factor is often determined in a single refinement cycle with fixed neutron positional and thermal parameters. Although the neutron parameters are not influenced by valence density features, scale factors refined by such a procedure may still be biased by the use of spherical-atom scattering factors.

Features of an electron density difference may be interpreted qualitatively in terms of bonding and lone-pair density, but an accurate experimental scale factor is necessary to make quantitative interpretation feasible. An experimental measurement may also help to unravel bias introduced in parameters refined from X-ray data using various models. Since scale factors from different refinements often vary by 10%, scale factor measurements accurate to within about 1% would be useful.

Two major difficulties encountered are measurement of the amount of material illuminated by the incident beam and the determination of the intensity of this beam. Three different methods have been used here.

In the first, developed by Burbank (1965), a small single crystal is bathed in a uniform area of the incident X-ray beam, which is the best common arrangement in single-crystal intensity measurements. The direct beam is measured at the crystal position with the aid of attenuators and a small aperture of accurately known cross section. The amount of material in the crystal contributing to the scattering is measured by weighing the crystal with a microbalance.

A second method, previously employed by Cooper, Larsen, Coppens & Giese (1973) uses a single-crystal

plate of uniform thickness large enough to intercept the entire direct beam. This technique requires measurement of the total beam intensity and the thickness of the plate, rather than the intensity per unit cross section and the volume of the crystal.

In the third method, intensities of powder samples are measured in the Bragg geometry. A number of the relevant experimental details have been discussed by Chipman (1969). The sample can easily be made large enough to intercept the entire direct beam. In the approximation of a sample of infinite thickness (James, 1965) the amount of material contributing to the scattering is a function of the absorption coefficient.

All of the compounds studied here have been the object of electron density investigations. A survey is given in Table 1.

Table 1. *Survey of compounds studied*

Compound	Method	Original study
Orthorhombic sulfur (Room temp.)	I, II, III	Blessing *et al.* (1973)
Orthorhombic sulfur (100°K)	I, III	Blessing *et al.* (1973)
α-Deutero-glycylglycine	I, II, III	Griffin & Coppens (1975)
α-Deutero-oxalic acid	I, II, III	Coppens *et al.* (1969).
Hexamethylene-tetramine	I, II, III	Stevens & Hope (1975*a*)
Sodium azide	I, II, III	Stevens & Hope (1975*b*)
Ammonium tetroxalate	I, III	Stevens (1973)

Samples

Samples for the small-single-crystal method and the powder method were prepared and crystallized as in the original studies. Partially deuterated glycylglycine and deuterated oxalic acid were prepared by repeated recrystallization from D_2O.

Growing suitable crystals for the single-crystal-plate method in some cases required considerable effort. Sodium azide crystals, which easily grow in large (0001) plates were always twinned, as were the smaller crystals used in the first method. Data were collected for both twins and combined in the same manner as in the previous study (Stevens & Hope, 1975*b*). Scale-factor measurements were made on two different NaN_3 plates. A (111) sulfur plate was obtained from CS_2 solution and a (001) plate from 1,1,2,2-tetrabromoethane (Groth, 1906). A (100) plate of HMT was obtained from the surface of an aqueous solution after evaporation of most of the solvent.

Method I. Small single crystal

In the absence of extinction, the integrated intensity measured on an absolute basis is given by (James, 1965)

$$\frac{E_s\omega}{I_0} = \frac{N^2\lambda^3}{\sin 2\theta}|F|^2\left(\frac{e^2}{mc^2}\right)^2 AVP. \qquad (4)$$

E_s is the total diffracted energy when the crystal passes through the reflection range with velocity ω in rad s^{-1}.
I_0 is the incident beam energy per unit area and unit time.
N is the number of unit cells per unit volume.
λ is the X-ray wavelength.
F is the absolute structure amplitude.
e^2/mc^2 is the classical scattering amplitude of a point electron.
θ is the Bragg angle.
A is the transmission factor.
V is the volume of the crystal.
P is the appropriate polarization factor.

Direct-beam measurement

The intensity of the direct beam at the crystal position was measured with an iridium aperture of 70 μm diameter as used in electron microscopy. The aperture was mounted on a goniometer head which allowed horizontal and vertical translations, and centered on a Picker diffractometer. Before each measurement, the aperture was oriented normal to the incident beam by maximizing the intensity with respect to rotation about horizontal and vertical axes. With an incident-beam collimator of 1·7 mm diameter, translation of the aperture established that the center of the direct beam was uniform to within 1·1 % over an area with a diameter of about 1·5 mm.

The cross-sectional area of the aperture was determined optically with a calibrated micrometer eyepiece.

The molybdenum X-ray tube was operated at 50 kV and 16 mA at a take-off angle of 2·5°. The incident-beam intensity was reduced using niobium foil attenuators. Attenuator factors and the detector dead time were calculated from measurements at various tube currents using a weighted least-squares fit to the linear function $R = R_t - N_0\tau(R_t - 1)$ (Chipman, 1969). Error estimates were derived from the variances of the least-squares fit.

Measurements of the direct beam were made before and after data collection with each sample. By translating the aperture, the intensity of the incident beam was averaged over an area of the beam coinciding approximately with the area intercepted by the crystal.

To check the wavelength dependence of the absorption by the Nb attenuator foils of unmonochromatized incident radiation, measurements were made on a small crystal of basic beryllium acetate both with and without an incident-beam graphite monocrhomator, while attenuation factors of the foils were remeasured using monochromatic radiation.

About 120 reflections of moderate intensity were measured with the monochromator in place, then remeasured with the monochromator removed. In each case the direct beam was also measured. After scaling, the root-mean-square deviation in intensities of the two sets was 1·3 %. The scale factor from the least-squares fit of the two data sets, combined with

measurements of the direct beam gave a total correction factor of 1·899 (9) in intensity. The standard deviation was calculated from estimates of the errors in the least-squares fitting procedure, errors in the direct-beam measurements from counting statistics and dead-time corrections, and errors in the attenuation factors. The correction factor was used to calibrate all of the direct-beam measurements.

The correction factor is smaller in this case than that in Method II (see below), but increases with decreasing take-off angle of the X-ray tube, indicating that without the monochromator, more divergent X-rays are allowed to enter the detector by the pinhole than by a crystal.

Crystal volume

The crystal volume was determined from the density by weighing the crystal with a Cahn electrobalance. Independent weighings of the crystal established that the precision of a single measurement was about 1·5 μg. Crystals with weights of about 200 μg or greater were chosen for measurement, and five or more measurements used to calculate the mean weight and the standard deviation of the mean. The accuracy of the weighings also depends on the accuracy of the Class *M* 1 mg standard weight used to calibrate the instrument. The stated accuracy of the 1 mg standard is $\pm$0·0054 mg.

Data collection

Intensity data were collected using a step-scan procedure (Blessing, Coppens & Becker, 1974) on a Picker FACS-1 automated diffractometer using Nb-filtered Mo $K\alpha$ radiation. Standard deviations were assigned to the intensity measurements based on counting statistics. The observed step-scan intensities were corrected for coincidence losses and the background was subtracted. Corrections for Lorentz and polarization effects were applied.

Dimensions of the crystal were carefully measured with a microscope and absorption corrections calculated by numerical integration over a Gaussian grid. For the sulfur single crystal, which had the largest absorption correction, the volume calculated from the dimensions agreed within 2% with the volume calculated from the crystal weight.

The scale factors were determined by fitting the structure factors measured on an absolute basis to the observed structure factors of the previous studies. The quantity $S=\sum w(kF_{\text{absolute}}-F_{\text{relative}})^2$ was minimized, where the weight of each observation was taken as $w=1/[k^2\sigma^2(F_{\text{absolute}})+\sigma^2(F_{\text{relative}})]$. The effects of extinction were minimized by discarding strong observations until no intensity-dependent systematic effects were apparent in the observations.

Low-temperature measurements were made with the cryostat system described by Coppens, Ross, Blessing, Cooper, Larsen, Leipoldt, Rees & Leonard (1974). For comparison with previous data, measurements on hexamethylenetetramine were corrected for included thermal diffuse scattering (TDS) using the program of Stevens (1974).

Method II. Single-crystal plate

For a large single-crystal plate, the integrated intensity on an absolute scale is given by (James, 1965)

$$\frac{E_{s(e)}}{I_0}=\frac{N^2\lambda^3}{\sin 2\theta}|F|^2\left(\frac{e^2}{mc^2}\right)^2\frac{t_0}{\cos\delta}AP. \qquad (5)$$

I_0 is the total energy in the direct beam per s.
t_0 is the thickness of the crystal plate.
δ is the angle between the incident beam and the crystal plate normal.

Direct-beam measurement

An incident-beam collimator of 0·5 mm diameter was used throughout the experiment. The intensity of the direct beam was attenuated with Nb foils. Attenuation factors were measured and the detector dead time determined as described for the small-single-crystal experiment. In this method, the detector dead time was smaller, since at a given intensity, the incident beam was spread out over a larger area of the detector crystal.

As with Method I, the attenuator factors measured using unmonochromatized radiation were in error owing to the wavelength-dependent absorption of the attenuator foils. Measurements on a large single-crystal plate of sulfur with and without a graphite monochromator were used to calibrate the direct-beam measurements. The data were collected and processed as described for Method I. The r.m.s. deviation in intensities of the two sets was 1·5%. Combining the scale factor from the least-squares fit of the two data sets with measurements of the direct beam with and without the monochromator gave a total correction factor of 25·01 (14) in intensity.

Plate thickness

The thickness of each plate was measured using the absorption of monochromatic Ti $K\alpha$ radiation. Attenuation factors were calculated from mass attenuation coefficients taken from *International Tables for X-ray Crystallography* (1974). In most cases, the thickness was also measured optically, or by measuring the surface area and weighing the crystal. From previous studies, (Cooper, Larsen, Coppens & Giese, 1973) measurements using the absorption of X-rays were considered to be the most reliable, and they are used here in all calculations. Results of various measurements are listed in Table 2.

Data collection

Intensity data were collected as in the single-crystal method. The angle δ between the incident beam and the crystal-plane normal, and the angle δ' between the diffracted beam and the plane normal were calculated along with Lorentz, polarization, and absorption cor-

Table 2. *Plate thickness measurements* (mm)

	Absorption*	Optical	Area & weight
Sulfur (R.T.)			
No. 1 (001)	0·266 (3)	0·280 (12)	0·261 (7)
No. 2 (111)	0·574 (4)	0·584 (13)	
α-Glycylglycine	0·0877 (10)	0·0871 (31)	
α-Oxalic acid	0·635 (4)	0·636 (12)	
Hexamethylene-tetramine	0·0135 (5)	0·0139 (6)	0·0130 (9)
Sodium azide			
No. 1 (0001)	0·0700 (10)	0·0711 (45)	0·0681 (22)
No. 2 (0001)	0·0528 (8)	0·0540 (70)	

* Uncertainty in the absorption coefficient not included in the estimated standard deviation.

rections for each reflection. Reflections with δ angles at which the plate might not intercept the entire direct beam were discarded, as were all reflections with either δ or δ' greater than 60°.

The absolute structure factors were fitted to the relative values as described above for the small-single-crystal method. Extinction was also treated in the same manner. For hexamethylenetetramine, intensity measurements were again corrected for TDS.

Model III. Powder

For a powder sample intercepting the entire incident beam in the symmetrical Bragg geometry (James, 1965),

$$\frac{E_s\omega}{I_0} = \frac{N^2\lambda^3}{\sin 2\theta \sin\theta}|F|^2\left(\frac{e^2}{mc^2}\right)^2\frac{pl}{16\pi\mu r}P. \quad (6)$$

p is the multiplicity of the reflection.
μ is the absorption coefficient of the sample.
l is the length of the detector slit.
r is the radius of the diffractometer.

Direct-beam measurement

Measurements were made on a Philips vertical powder diffractometer equipped with a scintillation detector and pulse-height analyzer. The X-ray source was a Cu tube operated at 20 kV and 32 mA. The incident-beam intensity was determined from direct beam scans using the detector. Continuous scans were made in both directions with background measurements taken at both ends of the scans. The intensity of the incident beam was attenuated with brass foils. Measurements at various tube currents were used to calculate attenuation factors of the foils and the detector dead time (Chipman, 1969). The attenuation of intensity was sufficient to reduce the coincidence losses to less than 1 % at the maximum counting rates.

Measurements of a Cu $K\beta$-wavelength reflection indicated that a correction of 1·31 (5) % was necessary for β radiation included in the direct-beam intensity.

Data collection

Intensities of the reflections were measured with Ni-filtered Cu $K\alpha$ radiation, continuous 2θ scans and stationary background measurements. The powder diffractometer has a diameter of 170·0 mm and the detector slit a length of 10·10 mm. Reflections were scanned repeatedly in both directions to reduce the uncertainty in intensity due to counting statistics to less than 1 %. When adjacent reflections or groups of reflections could not be resolved, the total intensity was measured and least-squares fitted to the sum of the corresponding relative intensities.

Most intensities measured were in the low-2θ range where reflections are well separated. It was assumed that extinction did not significantly influence the powder intensities. Extinction corrections for the original structure factors were taken as determined in the original X-ray refinement.

TDS corrections were calculated for the HMT powder data using a computing procedure modified for powder intensity measurements (Stevens, to be published).

Sample preparation

Specimens for data collection were prepared by grinding single crystals in an agate mortar or by mechanical grinding using a Wig-L-Bug. The powder was packed in rectangular sample holders using a procedure similar to the one described by McCreery (1949) to avoid preferred orientation.

Samples of sodium azide, which crystallized in (0001) plates showed some evidence of preferred orientation: the 000*l* reflections were stronger and the *hki*0 weaker than the corresponding single-crystal reflections after scaling. Higher standard deviations are obtained in the least-squares fitting procedure but a systematic error may be introduced as the reflections selected are not a random set.

Absorption factors were measured for each compound by placing the sample perpendicular to the incident beam. Measurements were averaged over translations of the sample. Measured attenuation factors were in good agreement with those calculated from mass attenuation coefficients tabulated in *International Tables for X-ray Crystallography* (1974) except for NaN_3 in which the measured value was somewhat higher.

Low-temperature measurements

A low-temperature sample holder was constructed for the Philips vertical powder diffractometer. The sample holder is brass with plastic foam insulation. Liquid nitrogen is forced through a Dewar tube into a chamber below the sample. The cooling of the evaporating nitrogen is balanced with heating applied with resistance wire embedded in the sample holder. Using a thermocouple mounted at the edge of the powder sample, voltage to the resistance heater was automatically adjusted to compensate for temperature changes. Temperature fluctuations were less than ±2·5°. Exiting nitrogen gas and 2 thin mylar sheets protected the sample from frost.

Experimental errors

The estimated contributions to the error in the scale factors for the room-temperature sulfur measurements are listed in Table 3. For Methods I and II, the direct-beam measurement contribution is estimated from counting statistics and stability of the source as reflected in the agreement of measurements before and after data collection. For Method III, a contribution from background measurements is also included.

Table 3. *Estimated errors for orthorhombic sulfur (room temperature)*

Small-single-crystal method I	Estimated % error (in k^2)
Direct-beam measurement	0·21 %
Dead-time correction	0·45
Attenuation factors (total)	0·66
Aperture area	0·68
Crystal volume	0·76
Least-squares fit to relative data set	0·61
Total	1·45 % (0·72 % in k)

Single-crystal-plate method II	Estimated % error (in k^2)
Direct-beam measurement	0·26 %
Dead-time correction	0·65
Attenuation factors (total)	0·87
Plate thickness	1·25
Least-squares fit to relative data set	0·94
Total	1·92 % (0·96 % in k)

Powder method III	Estimated % error (in k^2)
Direct-beam measurement	0·6 %
Coincidence loss	0·3
Attenuation factors (total)	0·9
Absorption coefficient	1·3
Slit length	0·2
Diffractometer radius	0·2
Least-squares fit to relative data set	1·5
Total	2·3 % (1·2 % in k)

The attenuation factor and dead-time correction contributions were calculated from their estimated standard deviations. The estimated errors in the direct-beam calibration measurements are included in the attenuation factor contributions for methods I and II. Similarly, for the powder method, the estimated error in the β-wavelength correction to the direct-beam intensity is included in the attenuation factor contribution. The coincidence-loss contribution in method III is calculated from the known dead time of the detector for the highest counting rate in scanning the direct beam.

The relatively large uncertainty in the measurements of the plate thickness results from lack of precision in the absorption coefficient rather than the reproducibility of the measurements. It has been estimated from the agreement with other methods of measuring the thickness. In the powder method, the effect of the uncertainty in the absorption coefficient has been estimated from agreement with experimental absorption measurements.

Further examination of Table 3 shows that major sources of error result from the determination of the amount of scattering material: measurement of the crystal volume (method I), of the plate thickness (method II) and of the absorption coefficient of the sample (method III). The precision of the powder intensity measurements, as reflected in the poorer least-squares fit to the single-crystal data is also a major contribution to the error in the powder measurement.

Results and discussion

Experimentally determined scale factors are listed in Tables 4–10 along with some scale factors from least-squares refinements. The scale of the data for sulfur at room temperature and at 100 °K differ by a factor 1·0962 introduced in data processing. With the unit-cell contraction of 0·9802 (5), this brings the scale-factor measurements at the two temperatures into agreement within the estimated standard deviations.

Table 4. *Orthorhombic sulfur (room temperature)*

X-ray refinements	
HF scattering factors	2·300 (5)
HF core, STO valence scattering factors	2·223 (5)
Refinements of scale only	
Neutron parameters, HF scattering factors	2·118 (4)
Neutron parameters, HF core, STO scattering factors	2·089 (3)
Experimental	
Small single-crystal	2·201 (16)
Single-crystal plate No. 1 (001)	2·170 (21)
No. 2 (111)	2·198 (22)
Powder	2·229 (45)

Table 5. *Orthorhombic sulfur* (100 °K)

X-ray refinements	
Full data, HF scattering factors	2·200 (3)
High-order data, HF scattering factors ($\sin\theta/\lambda > 0{\cdot}75$)	2·051 (25)
Refinements of scale only	
High-order X-ray parameters, HF scattering factors	2·129 (2)
Experimental	
Small single crystal	2·038 (18)
Powder	2·021 (55)

Table 6. *α-Deutero-glycylglycine*

X-ray refinements	
HF scattering factor	5·90 (1)
HF core, STO valence with refinement of Kappas and charges	5·62 (3)
HF core, STO valence with refinement of charges	5·54 (1)
Refinement of scale only	
Neutron parameters	5·55 (1)
Experimental	
Small single crystal	5·63 (8)
Single-crystal plate	5·49 (11)
Powder	5·58 (9)

Table 7. *α-Deutero-oxalic acid*

X-ray refinements	
HF scattering factors	0·841 (3)
HF core, STO valence scattering factors	0·775 (3)
Refinement of scale only	
Neutron parameters	0·819 (3)
Experimental	
Small single crystal	0·814 (9)
Single-crystal plate	0·810 (7)
Powder	0·821 (15)

Table 8. *Hexamethylenetetramine*

X-ray refinements	
HF scattering factors	
Low-order data (sin $\theta/\lambda < 0{\cdot}65$)	38·8 (1)
High-order data (sin $\theta/\lambda > 0{\cdot}65$)	35·7 (1)
HF core, STO valence scattering factors	
Low-order data	35·7 (1)
High-order data	35·8 (1)
Experimental	
Small single crystal	36·1 (3)
Single-crystal plate	36·0 (9)
Powder	36·1 (9)

Table 9. *Sodium azide*

X-ray refinements	
HF scattering factors	
Low-order data (sin $\theta/\lambda < 0{\cdot}65$)	35·4 (3)
High-order data (sin $\theta/\lambda > 0{\cdot}65$)	34·0 (1)
HF core, STO valence scattering factors	
Low-order data	35·2 (3)
High-order data	34·2 (1)
Refinements of scale only	
Neutron parameters	33·3 (1)
High-order X-ray parameters	34·4 (1)
Experimental	
Small single crystal	34·4 (4)
Single-crystal plate No. 1	33·9 (6)
No. 2	34·5 (5)
Powder	34·8 (7)

Table 10. *Ammonium tetroxalate*

X-ray refinements	
HF scattering factors	
Low-order data (sin $\theta/\lambda < 0{\cdot}65$)	8·72 (2)
High-order data (sin $\theta/\lambda > 0{\cdot}65$)	8·41 (4)
HF core, STO valence scattering factors	
Low-order data	8·16 (2)
High-order data	8·69 (5)
Refinement of scale only	
Neutron parameters	8·50 (3)
Experimental	
Small single crystal	8·45 (8)
Powder	8·52 (15)

For all of the structures studied, conventional X-ray refinements, in which low-order data are fitted to a spherical-atom model with HF scattering factors, yield scale factors which are too high when compared with experimental values. Since the X-ray atomic thermal parameters are known to show significant bias from molecular valence density features and are often highly correlated with the scale factor, it is reasonable to expect that bias is also introduced in the refined scale factor.

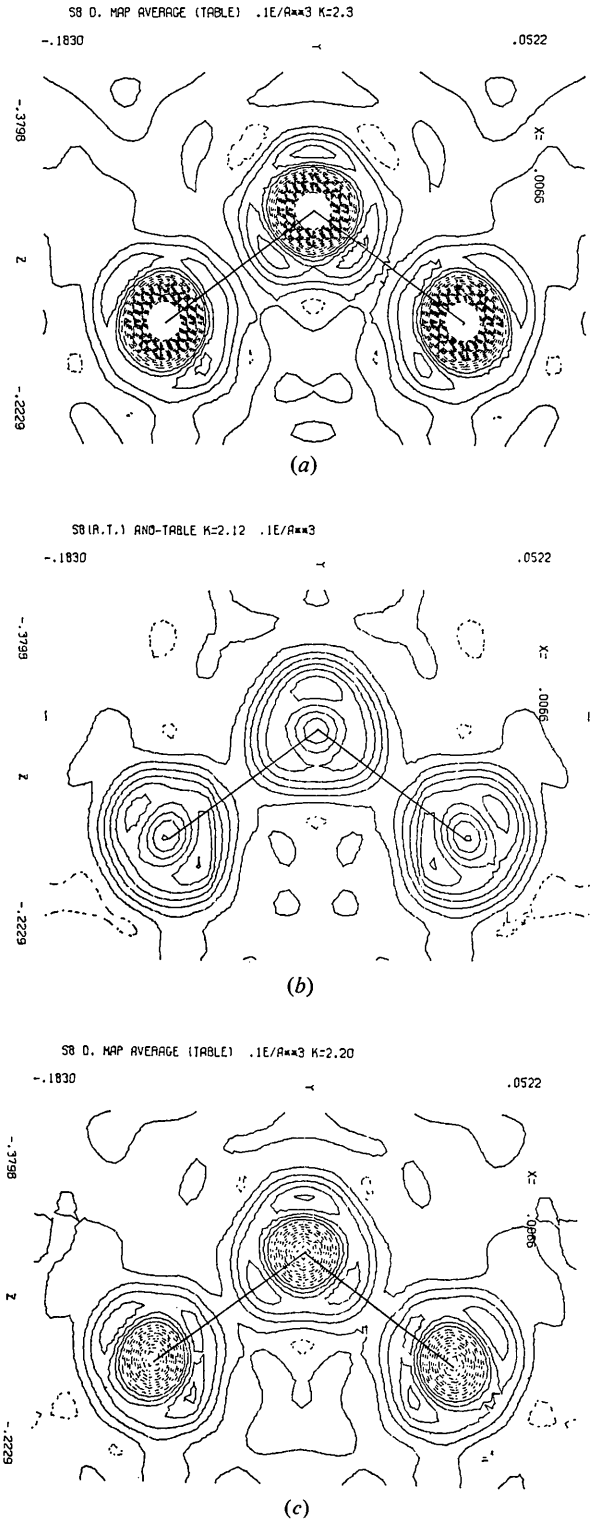

Fig. 1. Section of the S_8 ring containing three bonded sulfur atoms averaged over the four crystallographically unique planes: (*a*) ϱ(X–N) calculated with $k = 2{\cdot}30$ from the least-squares X-ray refinement; (*b*) ϱ(X–N) calculated with $k = 2{\cdot}12$ from a cycle of refinement with neutron parameters; (*c*) ϱ[X–N) calculated with the average experimental value of $k = 2{\cdot}20$. Contours are at 0·10 e Å^{-3}.

Parameters from refinement of high-order X-ray data are expected to show less bias, since the scattering at high angles is due primarily to core electrons. Scale factors from high-order refinements of sodium azide, hexamethylenetetramine, ammonium tetroxalate, and sulfur (100°K) are found to be in much better agreement with experimentally determined values.

Since the distribution of electrons around an atom in a molecule is likely to be expanded or contracted with respect to the isolated atom, refinements with improved scattering factors often yield parameters which show less bias from the molecular electron density distribution. When molecule-optimized STO rather than HF scattering factors are used, refined scale factors are in better agreement with the experimental values. Also, with glycylglycine, the scale factor from a *RADIAL* refinement, in which the angular dependences of the scattering factors are allowed to vary (Becker, Yang & Coppens, to be published), and the scale factor from an extended *L*-shell (ELS) refinement (Coppens, Pautler & Griffin, 1971), in which the populations of the valence shells are varied, are in better agreement with the experimental values. Of course, parameters from refinements using a spherical-atom model may still contain bias due to the asphericity of the electron density distribution.

Scale factors refined using fixed neutron parameters are generally in good agreement but often slightly lower than the experimental values. Although the parameters from neutron diffraction are not biased by the electron density features, the refined scale factor is influenced by the choice of X-ray scattering factors and by the use of a spherical-atom model.

Fig. 1 shows the effect of various scale factors on X–N difference density of orthorhombic sulfur at room temperature. The map is calculated in the plane of three neighboring sulfur atoms in the eight-membered ring and averaged over four crystallographically unique planes in the ring. Contours are at 0·10 e $Å^{-3}$.

Fig. 1(*a*) shows the difference density calculated with the scale factor from the conventional X-ray least-squares refinement using HF scattering factors. Large holes are observed at the nuclear positions. In Fig. 1(*b*), which is calculated using the scale factor from a cycle of refinement with fixed neutron parameters, the minima at the nuclear positions have all but disappeared. The map with the average of the experimentally determined scale factors [Fig. 1(*c*)] indicates that the earlier results are biased in opposite directions.

Fig. 2 gives a second example of the effect of the choice of scale factor. Fig. 2(*a*) shows the X–N difference density of the azide ion in the structure of NaN_3. The plane plotted contains the nitrogen nuclei along the threefold axis. The contours are at 0·05 e $Å^{-3}$. The scale factor used in the calculation was taken from the conventional low-order refinement with HF scattering factors.

Fig. 2(*b*) shows the same map calculated using the scale factor refined from a single cycle of least squares using the neutron parameters. Fig. 2(*c*) shows the map calculated with the average of the experimental scale factors.

Both these examples demonstrate the need for careful selection of the scale in any quantitative interpretation of density maps. It is obvious that the den-

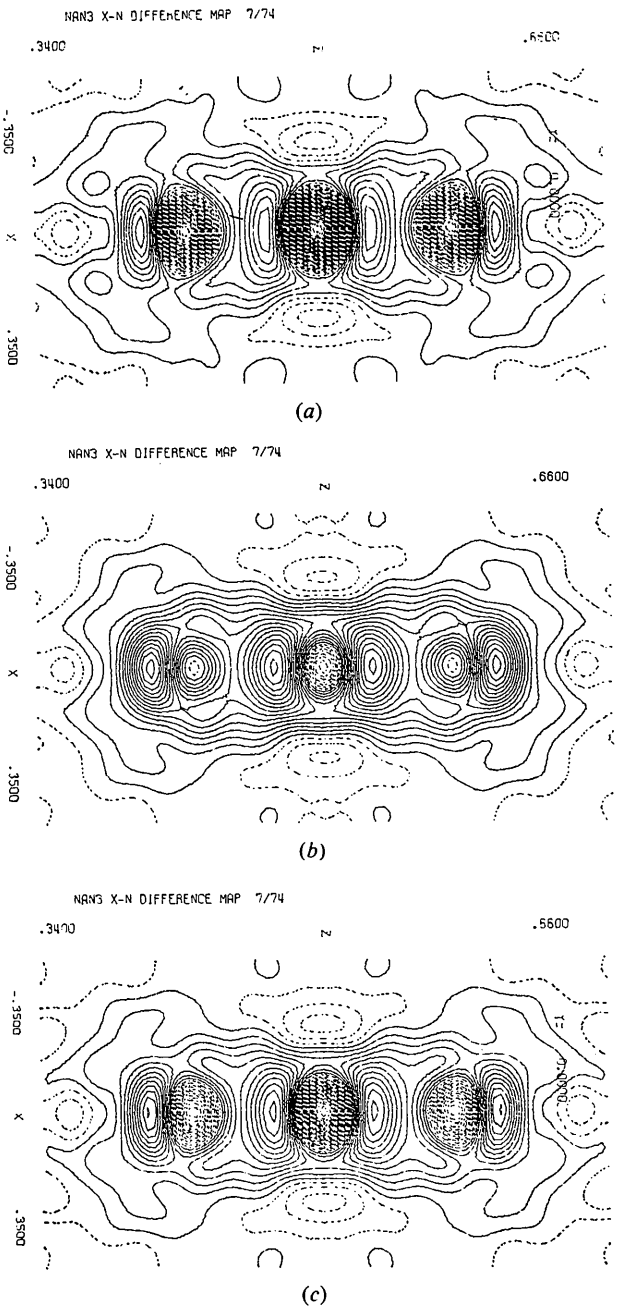

Fig. 2. Section containing the azide ion of NaN_3: (*a*) ϱ(X–N) calculated with $k=35{\cdot}4$ from low-order X-ray refinement; (*b*) ϱ(*D*–N) calculated with $k=33{\cdot}3$ from a cycle of refinement with neutron parameters; (*c*) ϱ(X–N) calculated with the average experimental value of $k=34{\cdot}4$. Contours are at 0·05 e $Å^{-3}$.

sities around the nuclei are totally unreliable without such a determination, in accordance with expression (3). The chemical interpretation of the density maps will be discussed in separate publications.

Conclusions

An estimate of the various errors indicates that scale factors can be measured with an accuracy of about 1%. Measurements using three methods agree within this error estimate.

Scale factors from conventional least-squares refinement are generally too large. Those obtained in a refinement with fixed neutron parameters are in better agreement with experimental values, but often somewhat low. Modified methods, such as refinement of high-order data, refinements with improved scattering factors, or refinements in which the shapes of the scattering factors are allowed to vary usually give scale factors in better agreement with the experimental scale factor, provided the accuracy of the data justifies such refinements. Such results should therefore be used instead of conventional scale factors in cases where experimental determinations of the absolute scale are impractical. However, a careful determination of the scale should be part of a charge density study, whenever feasible.

Support of this work by the National Science Foundation is gratefully acknowledge. We would also like to thank Dr A. D. Cadenhead for use of the electrobalance and Dr C. V. Clemency for making the X-ray equipment for the Ti $K\alpha$ absorption measurements available.

References

BLESSING, R. H., COOPER, W. F., YANG, Y. W. & COPPENS, P. (1973). *ACA Conf. Abs. Series* 2, **1**, 200.
BLESSING, R. H., COPPENS, P. & BECKER, P. (1974). *J. Appl. Cryst.* **7**, 488–492.
BURBANK, R. D. (1965). *Acta Cryst.* **18**, 88–97.
CHIPMAN, D. R. (1969). *Acta Cryst.* A**25**, 209–214.
COOPER, W. F., LARSEN, F. K., COPPENS, P. & GIESE, R. F. (1973). *Amer. Min.* **58**, 21–31.
COPPENS, P. (1974). *Measurement of Electron Densities in Solids by X-ray Diffraction.* MTP International Review of Science, Butterworths: London. In the press.
COPPENS, P. (1972). *Israel J. Chem.* **10**, 85–91.
COPPENS, P., PAUTLER, D. & GRIFFIN, J. F. (1971). *J. Amer. Chem. Soc.* **93**, 1051–1058.
COPPENS, P., ROSS, F. K., BLESSING, R. H., COOPER, W. F., LARSEN, F. K., LEIPOLDT, J. G. REES, B. & LEONARD, R. (1974). *J. Appl. Cryst.* **7**, 315–319.
COPPENS, P., SABINE, T. M., DELAPLANE, R. G. & IBERS, J. A. (1969). *Acta Cryst.* B**25**, 2451–2458.
GRIFFIN, J. F. & COPPENS, P. (1975). *J. Amer. Chem. Soc.* **97**, 3496–3505.
GROTH, P. (1906). *Chemische Kristallographie*, Vol. I, p. 27. Leipzig: Englemann.
International Tables for X-ray Crystallography (1974). Vol. VI. Birmingham: Kynoch Press.
JAMES, R. W. (1965). *The Optical Principles of the Diffraction of X-rays.* Ithaca: Cornell Univ. Press.
MCCREERY, G. L. (1949). *J. Amer. Ceram. Soc.* **32**, 141–146.
STEVENS, E. D. (1973). *Experimental Determination of Electron Density Distributions by X-ray Diffraction: Theoretical and Experimental Prerequisites.* Thesis, Univ. of California, Davis.
STEVENS, E. D. (1974). *Acta Cryst.* A**30**, 184–189.
STEVENS, E. D. & HOPE, H. (1975*a*). *Acta Cryst.* A**31**, 494–498.
STEVENS, E. D. & HOPE, H. (1975*b*). In preparation.
STEWART, R. F. (1970). *J. Chem. Phys.* **53**, 205–213.

Acta Cryst. (1975). A**31**, 619

X-ray Debye Temperature of Lead Nitrate

BY R. G. KULKARNI AND G. K. BICHILE

Department of Physics, Marathwada University, Aurangabad, Maharashtra, India

(*Received* 29 *January* 1975; *accepted* 24 *February* 1975)

The X-ray Debye temperature θ_M of lead nitrate has been determined to be 161 ± 6°K, by measurement of the temperature variation of the integrated intensities of Bragg reflexions from a powder specimen (method 1) in the temperature range 298–525°K. The room-temperature (298°K) Debye temperature for $Pb(NO_3)_2$ was determined to be 167 ± 6°K from integrated intensities of selected Bragg reflexions (method 2). Measured absolute structure amplitudes were used to calculate the root-mean-square displacements of the individual ions in $Pb(NO_3)_2$, which were found to be $0{\cdot}713 \pm 0{\cdot}099$ and $0{\cdot}326 \pm 0{\cdot}046$ Å for the Pb and $(NO_3)_2$ ions respectively.

1. Introduction

A number of physical parameters such as mean-square atomic displacements (Herbstein, 1961) and elastic constants (Gazzara & Middleton, 1964) are known to depend upon the Debye temperature of a solid. It has been shown by Salter (1965) that Debye temperatures obtained from different physical properties will not, in